

Preparation, characterization and dielectric study of new ferroelectric relaxors crystallizing with the tetragonal tungsten bronze structural type

M. Bouziane · A. Benabad · J. C. Niepce · B. Elouadi

Received: 25 June 2006 / Accepted: 18 April 2008 / Published online: 24 May 2008
© Springer Science + Business Media, LLC 2008

Abstract The replacement of sodium and niobium by lanthanum and iron in $\text{Pb}_2\text{NaNb}_5\text{O}_{15}$, have allowed to prepare the new solid state solution $\text{Pb}_2\text{Na}_{1-x}\text{La}_x\text{Nb}_{5-x}\text{Fe}_x\text{O}_{15}$ ($0 \leq x \leq 1$), crystallising with the tungsten bronze structure. The latter synthesized, in air, by solid state reaction, has been studied by means of X-ray and dielectric measurements. The composition dependencies of ferroelectric–paraelectric transition temperature and the lattice parameters are reported. The dielectric constants ϵ'_r and ϵ''_r have been also investigated as a function of temperature in the range 20°–700°C, and as a function of frequency in the range 1 k–13 MHz. In the composition range $0 \leq x \leq 0.35$, the materials exhibit a typical ferroelectric–paraelectric transition while, in the composition range $0.35 < x \leq 1$, a relaxor effect has been evidenced.

Keywords TB · Dielectric relaxor · Disorder · Ceramics

M. Bouziane (✉) · A. Benabad
Laboratoire de Chimie du Solide Appliquée,
Laboratoire Associé Francophone No. 501,
Faculté des Sciences, Avenue Ibn Batouta,
BP 1014 Rabat, Morocco
e-mail: bouzianemeryem@yahoo.fr

J. C. Niepce
Institut Carnot de Bourgogne, UMR 5209 CNRS,
Université de Bourgogne,
BP 47870, 21078 Dijon Cedex, France

B. Elouadi
Laboratoire d'Elaboration, d'Analyse Chimique et d'Ingénierie
des Matériaux, Département de Chimie,
Université de la Rochelle, avenue Michel Crépeau,
17042 La Rochelle Cedex 01, France

1 Introduction

Ferroelectric relaxor family materials exhibit interesting dielectric, electro-optical and non linear-optical properties. However, the relaxational behaviour well-known in lead-based perovskite compositions have been more recently reported in tungsten bronze ceramics [1–2].

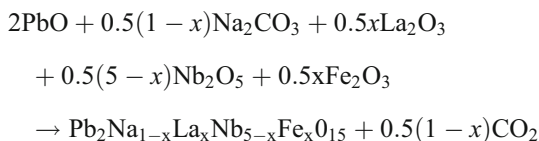
The tungsten bronze (TB) structure, deduced by Magneli [3], has a general formula $\text{A}_4\text{B}_2\text{C}_4\text{M}_{10}\text{O}_{30}$, consisting of octahedral MO_6 sharing corners delimiting three different types of sites 15 (A sites), 12 (B sites) and nine-fold (C sites) coordination. In these latter, various cations may enter and can influence the crystallographic and physical properties.

Recently, we have delimited a wide homogenous region within the triangle PbNb_2O_6 – $\text{Pb}_2\text{NaNb}_5\text{O}_{15}$ – $\text{Pb}_{1.875}\text{La}_{1.25}\text{Nb}_{3.75}\text{Fe}_{1.25}\text{O}_{15}$ crystallising with TB structural type in the ternary system PbNb_2O_6 – NaNbO_3 – LaFeO_3 [4] where only PbNb_2O_6 has the TB structure. In the present paper, the phase $\text{Pb}_2\text{Na}_{1-x}\text{La}_x\text{Nb}_{5-x}\text{Fe}_x\text{O}_{15}$ ($0 \leq x \leq 1$) belonging to determined TB field was chosen in order to check the evolution of crystal chemical and dielectric properties over the range $0 \leq x \leq 1$. Note that, the selected solid solution corresponds to the replacement of sodium and niobium by lanthanum and iron in $\text{Pb}_2\text{NaNb}_5\text{O}_{15}$. The results are discussed in comparison with relaxations in perovskite and TB-type ferroelectrics.

2 Experimental

All the compounds were synthesized, under air atmosphere, by heat treatment at 1100°C and 1200°C for ten hours, of PbO , Na_2CO_3 , Nb_2O_5 , Fe_2O_3 and La_2O_3 mixtures in the

stoichiometric proportions. The formation of the solid solution can be expressed by the following reaction:



The X-ray powder diffraction (XRPD) data were obtained with a classical diffractometer (C.G.R. Theta 60). The radiation was $\text{CuK}_{\alpha 1}$ selected by a quartz monochromator. Lattice constants for phase-pure samples were determined by scanning at $1/4^\circ/\text{min}$ using aluminium as an internal standard. The lattice constants were refined using a least-squares fit computer program.

The temperature dependence of the dielectric constants has been carried out in situ from room temperature up to 700°C at frequencies 10, 100 and 1000 kHz using HP4192ALF impedance spectrometer. The frequency dependence of the dielectric constants was studied in the frequency range 1 kHz to 13 MHz. Ceramic specimens were prepared as disks with 12 mm diameter and about 1 mm thick. They were fired at 1200°C for 4 hours and electroded by a silver paint.

3 Results

3.1 Crystalline characteristics

Based on XRPD, the $\text{Pb}_2\text{Na}_{1-x}\text{La}_x\text{Nb}_{5-x}\text{Fe}_x\text{O}_{15}$ compositions, all over the range $0 \leq x \leq 1$, were found to exhibit a single phase tungsten bronze structure. All diffraction lines were indexed using the non-centrosymmetric space group $\text{Cm}2\text{m}$ and the original lattice parameters of PbNb_2O_6 ($a=17.65 \text{ \AA}$, $b=17.92 \text{ \AA}$, $c=3.87 \text{ \AA}$) [5]. In Fig. 1, the variation of the lattice parameters and volume of unit cell with the composition is shown: a and c parameters changed very slightly while b parameter steeply decreased; so the b/a ratio became close to unity for values of $x \geq 0.4$. However, this result was not sufficient to decide whether the crystalline symmetry of the compositions with $0.4 \leq x \leq 1$ was orthorhombic or tetragonal. The unit cell volume is maintained almost constant. This result may be expected the fact that the ionic sizes of the cations incorporated [$r_{\text{La}(\text{sites } 12)}^{\text{I}} + r_{\text{Fe}(\text{sites } 6)}^{\text{I}} = 2.005 \text{ \AA}$ [6]] and those replaced [$r_{\text{Na}(\text{sites } 12)}^{\text{I}} + r_{\text{Nb}(\text{sites } 6)}^{\text{I}} = 2.03 \text{ \AA}$ [6]] are close together.

It is also worth to notice that the synthesis route for the stabilisation of the tungsten bronze structure is rather well defined for the title system. Therefore, initiation of even traces of the pyrochlore phase must be strictly avoided, because once this structure is formed, it is stabilised by all subsequent heat treatments and it becomes then impossible to isolate a pure

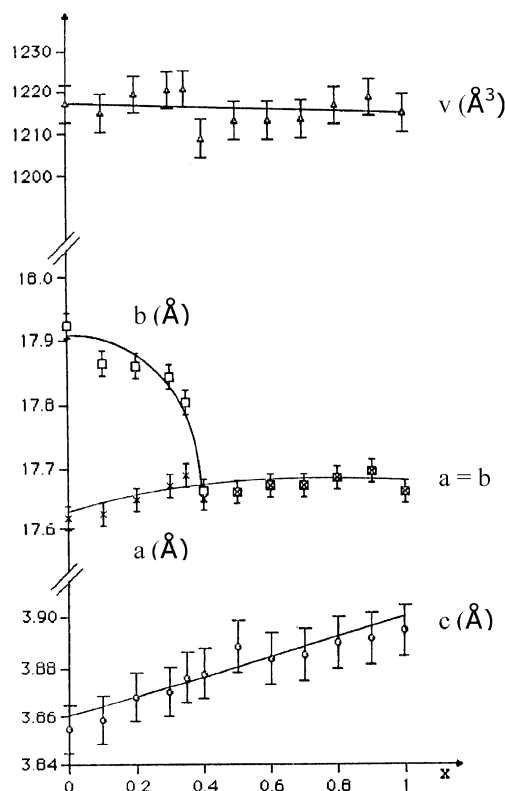


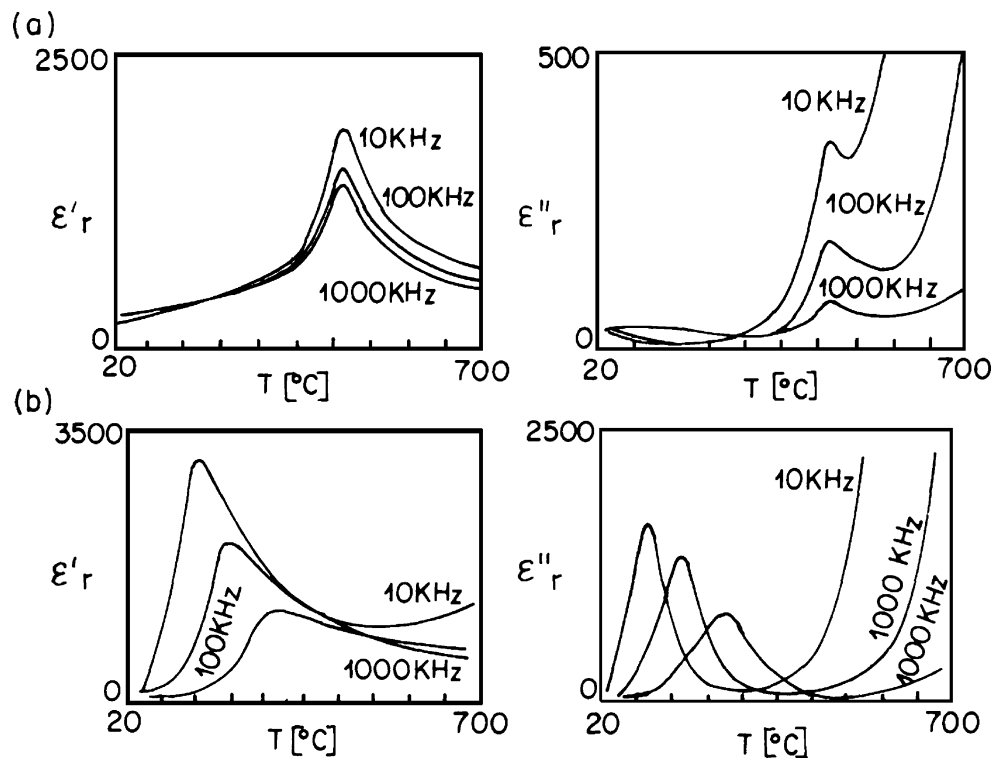
Fig. 1 Lattice parameters and the unit cell volume, at room temperature, versus x of $\text{Pb}_2\text{Na}_{1-x}\text{La}_x\text{Nb}_{5-x}\text{Fe}_x\text{O}_{15}$ ($0 \leq x \leq 1$)

and pyrochlore free tungsten bronze phase. Furthermore, low temperature sintering (at ca. 500°C for example) gives rise to pyrochlore phase. It is therefore highly recommended to submit the starting compounds mixture directly to high temperature ($T > 900^\circ\text{C}$) heat treatment, in order to isolate the whole range of the solid solution $\text{Pb}_2\text{Na}_{1-x}\text{La}_x\text{Nb}_{5-x}\text{Fe}_x\text{O}_{15}$ with the appropriate tungsten bronze structure. Similar behaviour has been encountered in the synthesis of $\text{Pb}_{0.5(5-x)}\text{La}_x\text{Nb}_{5-x}\text{Fe}_x\text{O}_{15}$ with the same structural type [7]. As reported by different authors, in the lead phases, the best procedure for obtaining samples with a single tungsten bronze structure seems to have a higher firing temperature in the first treatment [8, 9]. In the latter case, it is also required to achieve the first heat treatment of the starting mixture at a rather high temperature ($T > 900^\circ\text{C}$).

3.2 Dielectric measurements

The thermal variation of the dielectric constant has been investigated on ceramics of different compositions along the solid solution $\text{Pb}_2\text{Na}_{1-x}\text{La}_x\text{Nb}_{5-x}\text{Fe}_x\text{O}_{15}$ with $0 \leq x \leq 1$. A typical example of the thermal plots of ϵ_r' and ϵ_r'' is shown in Fig. 2 for two compositions of the system $\text{Pb}_2\text{Na}_{1-x}\text{La}_x\text{Nb}_{5-x}\text{Fe}_x\text{O}_{15}$ ($x=0.1$: $\text{Pb}_2\text{Na}_{0.9}\text{La}_{0.1}\text{Nb}_{4.9}\text{Fe}_{0.1}\text{O}_{15}$; $x=0.4$: $\text{Pb}_2\text{Na}_{0.6}\text{La}_{0.4}\text{Nb}_{4.9}\text{Fe}_{0.4}\text{O}_{15}$). For all investigated compositions, the Curie temperature T_C , is deduced from the peaks recorded on

Fig. 2 Relative permittivities ϵ'_r and ϵ''_r versus T of $\text{Pb}_2\text{Na}_{1-x}\text{La}_x\text{Nb}_{5-x}\text{Fe}_x\text{O}_{15}$ for three different frequencies 10, 100 and 1000 kHz: (a) $x=0.1$, (b) $x=0.4$



this type of graphs. The analysis of the T_C change versus composition allows the following conclusions:

(i) In the range $0 \leq x \leq 0.35$, both $\epsilon'_r(T)$ and $\epsilon''_r(T)$ plots exhibit sharp maxima at exactly the same temperature although the frequency is varied within a very large domain. The transition temperature appears then as frequency independent. However, as expected the intensity of the dielectric peaks decreases with increasing frequency values. Such behaviour is characteristic of regular ferroelectric materials. Figure 3 illustrates the change of T_C versus composition. It also shows a rather important decrease of T_C as the solid solution progresses along the system $\text{Pb}_2\text{Na}_{1-x}\text{La}_x\text{Nb}_{5-x}\text{Fe}_x\text{O}_{15}$. Similar results have been reported for equivalent materials where a T_C decrease was attributed to the replacement of niobium (V) by other cations [10]. The T_C diminution versus composition evidenced in Fig. 3 could be also interpreted as a result of a cationic valence change given by doping. As a matter of fact, such behaviour is predictable according to Subbarao and Hrizo who suggested that the substitution in a ferroelectric lattice of any parent ion with another of different valence state will give rise to a decrease of T_C [11].

(ii) On the contrary, over the range $0.35 < x \leq 1$, the dielectric behaviour is rather complex (Fig. 2(b)). The main features may be listed as follows:

- a diffuse phase transition behaviour,
- an important frequency dependence: the maximum of the dielectric constant peak shifts to higher temper-

- atures and decreases in magnitude with increasing frequency,
- a strong influence of the thermal history; as a consequence, a rather bad reproducibility, of the dielectric constant measurements, has been observed.

Such dielectric response looks very similar to relaxor behaviour.

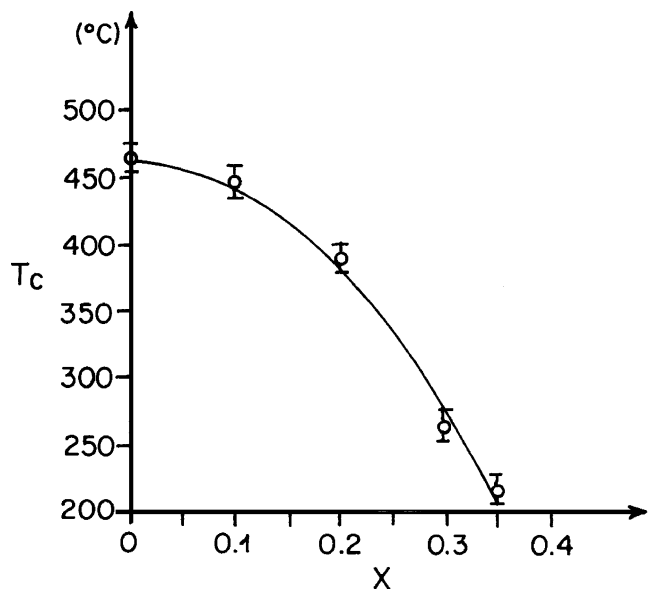


Fig. 3 Variation of Curie temperature versus composition x ($0 \leq x \leq 0.35$) for the system $\text{Pb}_2\text{Na}_{1-x}\text{La}_x\text{Nb}_{5-x}\text{Fe}_x\text{O}_{15}$

As shown in Fig. 4, a relaxation effect is also confirmed from the variation of the real and the imaginary parts ϵ'_r , ϵ''_r of the dielectric constant versus frequency (F) at room temperature [12]. Furthermore, the analysis of these plots evidences:

- (i) A broad peak $\epsilon''_r=f(F)$ whose maximum (corresponding to a displaced maximum of $D=f(F)$) coincides with an inflexion point on the graph $\epsilon'_r=f(F)$.
- (ii) The frequency dependence of ϵ'_r results in a decrease from a static value ϵ_0 at low frequencies, to a smaller limiting value ϵ_∞ at high frequencies.

Similar behaviour has already been observed in compounds with TB structure. The solid solutions $\text{Pb}_{0.5(5-x)}\text{La}_x\text{Nb}_{5-x}\text{Fe}_x\text{O}_{15}$ ($0 \leq x \leq 1$) [6] and $\text{Sr}_{2-x}\text{K}_{1+x}\text{Nb}_5\text{O}_{15-x}\text{F}_x$ ($0 \leq x \leq 1$) [13] show a relaxor effect only for highest values of x . Another example, two compositions belonging to the $\text{Pb}_{5-x}\text{K}_{6(1-x)}\text{Li}_{4(1-x)}\text{Ta}_{10}\text{O}_{30}$ solid solution present a different ferroelectric compartment. The first composition, $\text{Pb}_{2.5}\text{K}_3\text{Li}_2\text{Ta}_{10}\text{O}_{30}$ shows a classical ferroelectric behaviour; in contrast the second one $\text{Pb}_{3.75}\text{K}_{1.5}\text{LiTa}_{10}\text{O}_{30}$ shows a relaxor behaviour [14].

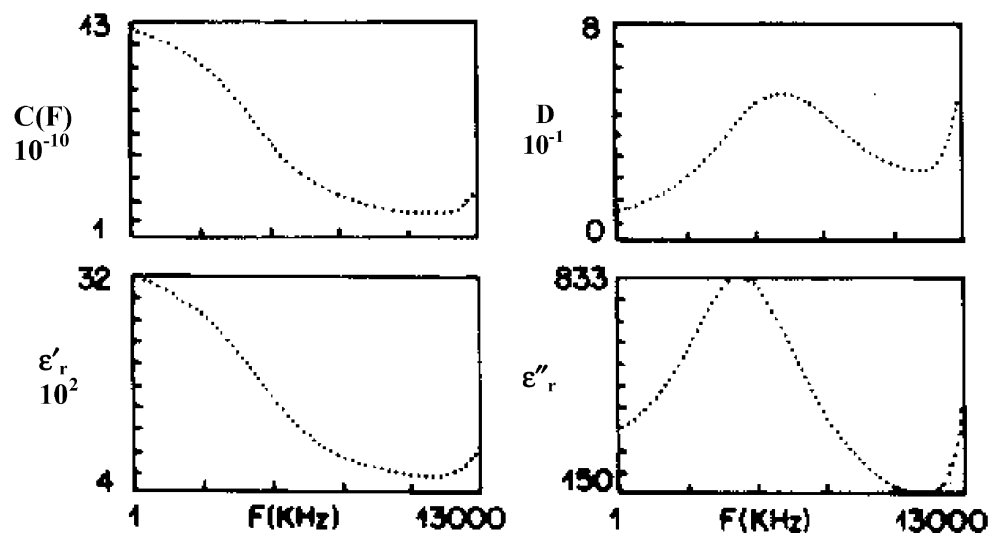
However, the dielectric relaxation is distributed over a wide frequency range. Therefore, the Cole and Cole representation seems to be more adapted to the observed relaxational behaviour [15]. A typical example of such a representation is given in Fig. 5 for a ceramic corresponding to the composition $\text{Pb}_2\text{Na}_{0.6}\text{La}_{0.4}\text{Nb}_{4.6}\text{Fe}_{0.4}\text{O}_{15}$ ($x=0.4$ in the title formula). The Cole and Cole plot results in a circular arc with centre situated below ϵ'_r axis. The observed departure from the Debye's theory suggests that the dispersion mechanism as proposed by Cole and Cole, is equivalent to a complex impedance in the equivalent circuit and is consequently not of a purely dissipating character [15].

On the other hand, ϵ'_r and ϵ''_r data were reported in Fig. 6, measured for the $x=0.4$ ceramic and obtained at various temperatures between 20° and 200°C, over the frequency range 1 kHz–13 MHz. It has to be noted that the departure from the semicircle observed in Fig. 6 is found at sufficiently high frequencies and increases strongly with the temperature. The particularities of dielectric data seem to be related to effects of intrinsic material properties and the ionic contributions to the electric transport play an important role.

4 Discussion and conclusion

Dielectric relaxation in ferroelectric materials occurs over a wide frequency range from 10^2 to 10^{12} Hz depending on the type of chemical or physical defects. The relaxors constitute a particular class characterized by specific dielectric properties as diffuse transition and dielectric relaxation $f_r < 10^7$ Hz observed only in ferroelectric phase [16]. The relaxor properties appear mainly in oxygen octahedron families like perovskite and tungsten bronze structures compositions. Various models have been proposed to explain the origin of the relaxor character. Particularly, in Smolenski model [17, 18], the relaxation is interpreted by a composition fluctuation resulting from cation disorder caused by ions of different valency located on crystallographically equivalent sites. In the Cross model [19], the relaxor behaviour is correlated with a cluster size effect. In 1990, Randall et al. [20] related the relaxor properties to the existence of nanoscale ordered domains in a disordered matrix. The common point in these models is the resulting break in symmetry who leads to a non long-range polar state, as is the case in classical ferroelectrics. In Tungsten bronze type, the relaxor behaviour is closely related to compositional hetero-

Fig. 4 Frequency dependence of ϵ'_r , ϵ''_r , the capacity C and loss factor D (ϵ''_r/ϵ'_r) of $\text{Pb}_2\text{Na}_{0.6}\text{La}_{0.4}\text{Nb}_{4.6}\text{Fe}_{0.4}\text{O}_{15}$



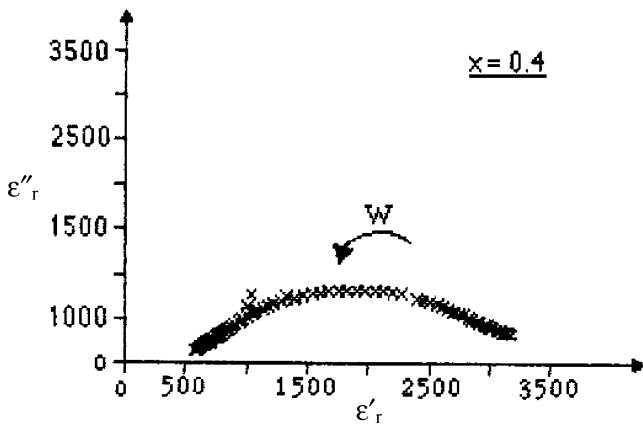


Fig. 5 Cole–Cole plot of $x=0.4$ ($\text{Pb}_2\text{Na}_{0.6}\text{La}_{0.4}\text{Nb}_{4.6}\text{Fe}_{0.4}\text{O}_{15}$)

generality in solid solutions and/or to order disorder nanostructures. In fact, Hornebecq and co-workers, in order to investigate the origin of the relaxor behaviour in the $\text{Pb}_5\text{Ta}_{10}\text{O}_{30}\text{--Li}_{10}\text{Ta}_{10}\text{O}_{30}\text{--K}_{10}\text{Ta}_{10}\text{O}_{30}$ ternary system, show that in the relaxor composition two conditions are verified [14]. The first condition, necessary but not sufficient, is the presence of two different cations in the same crystallographic sites. The second ones, the A sites (coordination number 15) is at least half occupied by lead atoms. Indeed, the relaxor behaviour is often associated to the presence of lead because of their high polarizability and non-engaged electron doublet. Other examples of tungsten bronze type relaxor ferroelectrics are given in literature: $\text{BaNa}_2\text{Nb}_5\text{O}_{14}\text{F}$ [21] (A sites is half occupied by Ba^{2+} and Na^+), $\text{Sr}_{1-x}\text{Ba}_x\text{Nb}_2\text{O}_6$ [22] (relaxation phenomena depend on the strontium content), $\text{Sr}_{2-x}\text{K}_{1+x}\text{Nb}_5\text{O}_{15-x}\text{F}_x$ [13] (relaxor behaviour resulting from ionic disorder observed for high value of x), etc...

In the present work, the relaxor behaviour lying between $10^4\text{--}10^5\text{Hz}$, is observed at $0.35 < x \leq 1$. In the light of results of the literature described above, it seems reasonable to expect such behaviour in $\text{Pb}_2\text{Na}_{1-x}\text{La}_x\text{Nb}_{5-x}\text{Fe}_x\text{O}_{15}$ compounds particularly for high values of x . For all compositions of the title solid solution, smaller trigonal section (C sites) are assumed to be totally free, since the probability of locating large ions is higher in large sites than in smaller ones. Thus, with increasing x , two cation dispersion types appear on octahedral sites (M sites) and tetragonal or pentagonal tunnels (A or B sites). Consequently, the condition corresponding to the presence of two different cations in the same crystallographic sites is verified. Moreover, four Pb^{2+} ions by unit-cell imply necessarily that the pentagonal sites are at least half occupied by lead ions. So, according to Hornebecq's model, conditions for existence of relaxor behaviour are satisfied. All these results are compatible with an increasing cationic disorder as the solid solution progresses from $x=0.0$ to $x=1.0$. As a consequence of the composition fluctuation, each local compositional zone will be characterised by a Curie

temperature different from that of the adjacent domain. The overall result is a broadened phase transition. On the other hand, for highest values of x , both La^{3+} and Fe^{3+} ions play the role of defect in the original $\text{Pb}_2\text{NaNb}_5\text{O}_{15}$ matrix. The resulting disorder perturbs the long range polarisation giving the ferroelectric relaxor behaviour.

In the course of studying ferroelectric compounds and solid solutions, some of them have been discovered to exhibit a morphotropic phase boundary (MPB). MPB ferroelectrics materials are well-known to possess enhanced physical properties because of the proximity of alternate ferroelectric states. Some of such compounds are $\text{Pb}(\text{Ti,Zr})\text{O}_3$, $\text{Pb}(\text{Mg}_{1/3}\text{Nb}_{2/3})\text{O}_3\text{--PbTiO}_3$ and $\text{Zn}_{1/3}\text{Nb}_{2/3}\text{O}_3\text{--PbTiO}_3$. A common factor in the temperature–concentration phase diagram of these compounds is the presence of a MPB which separates the rhombohedral phase from the tetragonal one [23, 24]. Nothing that, these latter present the relaxation properties. In TB structure, well-known example is lead barium niobate $\text{Pb}_{1-x}\text{Ba}_x\text{Nb}_2\text{O}_6$, which has a MPB at $x=0.37$ and separates two ferroelectric phases, tetragonal 4 mm and orthorhombic $m2m$ [25, 26]. Other MPB compositions have been found from the binary combination of bronze end-member phases such as PbNb_2O_6 , $\text{Pb}_2\text{KNb}_5\text{O}_{15}$, $\text{Sr}_2\text{NaNb}_5\text{O}_{15}$ and $\text{Ba}_2\text{NaNb}_5\text{O}_{15}$ [27–29]. In the present case, the variation of lattice parameters with composition (Fig. 1) did not permit at $x \geq 0.4$ a choice between tetragonal and orthorhombic symmetries. As MPB separates two ferroelectrics phases having distinct crystal-line symmetries and all compositions near MPB exhibit a relaxor behaviour around dielectric permittivity peak, it seemed to us reasonable to suspect the existence of a morphotropic phase boundary near the $x=0.4$. However, in the present situation, additional structure information is needed to support, complement and confirm such property. This work is now in progress in order to give an unambiguous conclusion about the close relation that may

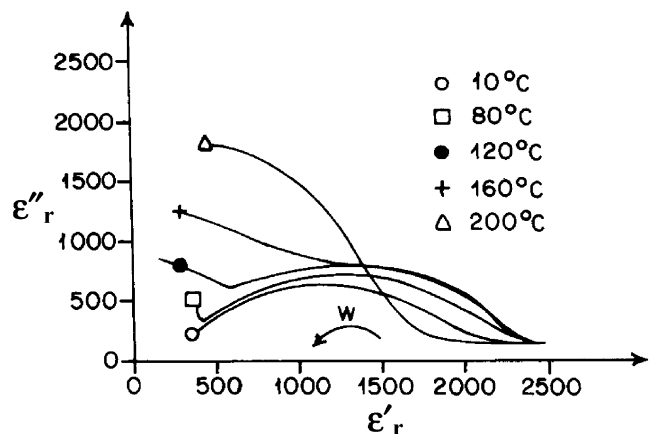


Fig. 6 Cole–Cole plot of $\text{Pb}_2\text{Na}_{0.6}\text{La}_{0.4}\text{Nb}_{4.6}\text{Fe}_{0.4}\text{O}_{15}$ ($x=0.4$) at various temperatures between 20° and 200°C

exist between the structural defects and the relaxor aspect of the analysed materials.

References

1. J.M. Povoia, R. Guo, A.S. Bhalla, *Ferroelectrics*, **158**, 283 (1994)
2. P. Sciau, Z.G. Lu, G. Calvarin, T. Roisnel, J. Ravez, *Mater. Res. Bull.*, **28**, 1233 (1993)
3. A. Magnéli, *Arkiv. Kemi.*, **24**, 213 (1949)
4. Bouziane, A. Benabad, J. C. Niepce and B. Elouadi, (to be published)
5. P.H. Labbe, M. Frey, G. Allais, *Acta Crystallogr.*, **B29**, 2204 (1973)
6. R.D. Shannon, C.T. Prewit, *Acta Crystallogr.*, **A. 32**, 751 (1976)
7. M. Bouziane, A. Benabad, J.C. Niepce, B. Elouadi, *J. Physique IV*, **123**, 177 (2005)
8. V.G. Krysh-top, R.U. Devlikanova, E.G. Fesenko, *Neorg. Mater.*, **15**(12), 2257 (1979)
9. T. Ikeda, K. Uno, K. Oyamada, A. Sagara, J. Kato, S. Takano, H. Sato, *Jpn. J. Appl. Phys.*, **17**, 341 (1978)
10. J. Ravez, A. Perron-Simmon, P. Hagenmuller, *Ann. Chim.*, **t1**, 251 (1976)
11. E.C. Subbarao, J. Hrizo, *J. Am. Ceram. Soc.*, **45**(11), 528 (1962)
12. J.C. Anderson, *Diélectriques* (Dunod, Paris, 1966), p. 50
13. H. El Alaoui-Belghiti, A. Simon, P. Gravereau, A. Villesuzanne, M. Elaammani, J. Ravez, *Solid State Sci.*, **4**(7), 933 (2002)
14. V. Hornebecq, C. Elissalde, F. Weil, A. Villesuzanne, M. Menetrier, J. Ravez, *J. Appl. Crystallogr.*, **33**, 1037 (2000)
15. K.S. Cole, R.H. Cole, *J. Chem. Phys.*, **9**, 341 (1941)
16. C. Elissade, J. Ravez, *J. Mater. Chem.*, **11**, 1957 (2001)
17. G.A. Smolensky, V.A. Isupov, A.I. Agranovskaya, S.N. Popov, *Soviet Phys-Solid State*, **2**, 2584 (1961)
18. G. Smolensky, *Ferroelectrics*, **53**, 129 (1984)
19. L.E. Cross, *Ferroelectrics*, **76**(12), 241 (1987)
20. C.A. Randall, A.S. Bhalla, *Jpn J. Appl. Phys.*, **29**, 327 (1990)
21. H. El Alaoui-Belghiti, A. Simon, M. Elaammani, J.M. Reau, J. Ravez, *Phys. Status Solidi (a)*, **187**(2), 549 (2001)
22. A.M. Glass, *J. Appl. Phys.*, **40**(12), 4699 (1969)
23. S.W. Choi, T.R. Shrout, S.J. Tang, A.S. Bhalla, *Ferroelectrics*, **100**, 29 (1989)
24. J. Kuwata, K. Uchino, S.N. Omoura, *Ferroelectrics*, **387**, 579 (1981)
25. T.R. Shrout, L.E. Cross, D.A. Hukin, *Ferroelectr. Lett. Sect.*, **44**, 325 (1983)
26. R. Guo, A.S. Bhalla, C.A. Randall, L.E. Cross, *J. Appl. Phys.*, **67**, 6405 (1990)
27. J. Ravez, A. Perron-Simon, B. Elouadi, L. Rivoallan, P. Hagenmuller, *J. Phys. Chem. Solids*, **37**, 949 (1976)
28. J.R. Oliver, R.R. Neurgaonkar, G.L. Shoop, *IEEE International Symposium on Applications of Ferroelectrics Berthlehem, PA, USA* 1986.
29. M. Marutake, M. Yokosuka, *Ferroelectrics*, **21**, 425 (1978)